# Linking Acoustic Communications and Network Performance: Integration and Experimentation of an Underwater Acoustic Network

Andrea Caiti, *Member, IEEE,* Knut Grythe, Jens M. Hovem, Sergio M. Jesus, Arne Lie, Andrea Munafò, *Member, IEEE,* Tor Arne Reinen, Antonio Silva, Fred Zabel

**Abstract**

Underwater Acoustic Networks (UANs) are an emerging technology for a number of oceanic applications, ranging from oceanographic data collection to surveillance applications. However, their reliable usage in the field is still an open research problem, due to the challenges posed by the oceanic environment. The FP7 UAN project moved along these lines, and it was one of the first cases of successful deployment of a mobile underwater sensor network integrated within a wide-area network, which included above water and underwater sensors. This contribution together with a description of the underwater network, aims at evaluating the communication performance, correlating the variation of the acoustic channel to the behaviour of the entire network stack. Results are given based on the data collected during the UAN11 sea trial. During the experimental activities, the network was in operation for five continuous days and was composed of up to four fixed nodes, two autonomous underwater vehicles and one mobile node mounted on the supporting research vessel. Results from the experimentation at sea are reported in terms of channel impulse response and signal to noise plus interference ratio as measured by the acoustic modems during the sea tests. The performance of the upper network levels are measured in terms of round trip time and probability of packet loss. The analysis shows how the

Andrea Caiti and Andrea Munafò are with the Inter-univ. Ctr. on Integrated Systems for the Marine Environment, Research Ctr. E. Piaggio, University of Pisa, Pisa, Italy.

Sergio M. Jesus, Antonio Silva and Fred Zabel are with the Institute for Systems and Robotics, University of Algarve, Faro, Portugal.

Knut Grythe, Jens M. Hovem, Arne Lie and Tor Arne Reinen are with SINTEF, Trondheim, Norway.

communication performance was dominated by variations in the SNR, and how this impacted on the behaviour of the whole network. Qualitative explanation of communication performance variations can be accounted, at least in the UAN experiment, by standard computation of Channel Impulse Response and Transmission Loss Estimate.

# Linking Acoustic Communications and Network Performance: Integration and Experimentation of an Underwater Acoustic Network

## I. Introduction

The on-going increase in reliability and performance of acoustic modems devices is paving the way to the development of mobile underwater sensor networks [1], [2], characterized by many autonomous sensing units, either fixed or mobile, by distributed sensing and data processing, by adaptivity (re-configuration, re-deployment, etc.) on the basis of locally sensed data and information available from other nodes through a communication infrastructure. Underwater Acoustic Networks (UANs) are an emerging technology for oceanographic data collection, pollution monitoring, offshore exploration and tactical surveillance applications. However, the transition from theoretical or proof of concept experiment to operational application in the underwater domain poses tougher challenges with respect to the terrestrial or aerial counterparts. The unique characteristics of the underwater acoustic channel make the efficient design of network models challenging, and their reliable implementation still an open research field. The major challenge in underwater application of autonomous cooperating sensing networks is still represented by node communication. In fact, the intrinsic limitations in bandwidth, time delay, channel fluctuation, imposed by the physics of acoustic propagation, have constrained so far the reliable set-up of communication infrastructures for sensor networks [3], [4], [5]. A theoretical overview of recent protocols for underwater networks is reported in [6], where the authors highlight the main drawbacks of most of the current acoustic network designs for robust and efficient UANs. As a result, underwater acoustic networks are still characterized by very large propagation delays, extremely low P2P data rates, high raw bit error rate (BER) and by frequent disruption of the communication links. Furthermore, field examples of UANs with measured performance in the field are scarce. An initial attempt to establish a UAN was conducted in 1998 with the Seaweb

experiments [7], with the aim of improving acoustic modems, originally developed for P2P communications, for usage within UANs. During the same project, Medium Access Control (MAC) and routing protocols were investigated for networks composed of underwater fixed nodes and gateways. The Seaweb experiments aimed at demonstrating the capability of UANs for surveillance operations. The experimental testing of an underwater network with mobile nodes and gateways is reported in [8], in the context of mine countermeasures applications. The deployed network was based on the OSI 7-layer model from the application to the physical layers. More recent results are available for one-to-many broadcasting [9], or for partial network implementation, as in [10]. Scarcity of results are, however, also due to the complexities of at-sea experimentations.

The UAN - Underwater Acoustic Network - project, funded by the European Union under the FP7 Programme, moved along these research lines and it has ended up in a successful deployment of a mobile underwater sensor network (UANp) integrated within a Wide-Area Network (WAN), which included above water and underwater sensors, for protection and security. The development of the UANp network was mostly based on known communication and network protocols, with the idea of a bottom-up approach, where each network layer can be finely tuned and adapted to perform optimally and as robust as possible when operating in the worst possible conditions of high packet loss or network link failures. The UANp structure included a physical and logic network layer, an IP layer, a Middleware layer capable of including network security features [11], and an application layer from where an operator was able to command and control the network.

The fundamental idea behind UAN approach is to maintain a desirable level of performance through adaptation of the network geometry to the physical acoustic propagation conditions at the particular time and water volume where the system is deployed. It is of relevance to emphasize the context in which the networked communication took place. In case of UAN, the context is that of an integrated security system for a coastal/offshore critical infrastructure, including aerial and surface devices and with a centralized command and control station; in this setting, the mobile nodes, placed on Autonomous Underwater Vehicles (AUVs), have the dual role of providing multi-hop capabilities guaranteeing the connectivity of the fixed nodes, and also of long range detection/inspection of possible intruders.

The UANp network [12] was fully deployed in May 2011, in the Trondheim Fjord area, Norway,

and operated for five continuous days during the UAN11 experimental activities. The network was composed of three mobile nodes, two fixed nodes and one gateway access point node (STU) [13], which being connected to shore with a fiber optic cable, represented the integration point between the underwater network and the above water surveillance system. On shore, and connected to the STU, the main data processing and the Command and Control (C2) station were installed. During the experimental activities, the network was fully operated and the whole security system tested in fictitious threat scenarios with AUVs patrolling the area and performing interception missions [14]. The C2 was receiving information and sending commands to any asset in the field using the acoustic network, as for example, to receive environmental data from fixed nodes, to move mobile nodes to different locations, etc. Furthermore, a uni-directional high data-rate link [**?**] from the remote nodes to a Vertical Hydrophone Array (VLA), located at the gateway access point node, was integrated with the network and used to transmit critical information (e.g. threat detection).

Together with the description of the specific design choices of the UANp network, the work presented in this paper aims at analysing the performance at different levels of the network. This analysis, based on the results measured in the field during the UAN11 sea trial, shows how the communication performance of UANp was dominated by the Channel Impulse Response (CIR) and by the Signal-to-Noise Ratio (SNR), while the modems were able to handle the presence of multipaths. This allows to directly correlate, at least some of the observed network performance with the environmentally driven acoustic characteristics of the channel data features. This is shown in the paper through channel simulations with the BELLHOP ray-code model [15].

The network communication performance has been evaluated at different levels using complementary metrics: the performance of the physical level are reported in terms of Channel Impulse Response (CIR), Signal-to-Noise plus Interference Ratio (SNIR) and packet reception ratio; the operation of the upper layers is evaluated with statistics on the Round Trip Time (RTT) and on the Packet Loss (PL) at IP layer, MOOS middleware and application level.

The paper is organized as follows: the next Section describes the UANp network topology and structure in details. Section III describes the UAN11 sea trial. The main environmental data measured at UAN11 are reported in Section IV. Section V goes into the details of the

main experimental results. In this section the network communication performance is described from the physical level up to the middleware and application levels. In Section VI we use the environmental data measured during the sea trial to feed the BELLHOP acoustic code to show how the channel impulse response (CIR) and the transmission loss changed between the nodes of the network as the oceanic conditions changed. Section VII is devoted to remarks and observations on the achieved communication performance. Finally, conclusions are drawn in Section VIII.

## II. Network structure and topology

The UANp network is a component of a wide area network, which includes above water and underwater sensors, for surveillance and protection of coastal and off-shore critical infrastructures. The integration point between the underwater and the above water part of the system is represented by an underwater base station (STU - Subsurface Telemetry Unit) connected to shore with a high bandwidth link (e.g. fiber optic cable), and which is both a part of the acoustic network and of a traditional wired communication infrastructure. The underwater network is composed of acoustically connected fixed and mobile nodes, which act both as communication nodes and as surveillance and reactive assets for protection. A land station, acts as a Command and Control (C2) center to monitor and to coordinate the physical defence of the infrastructure. The complete UANp system is hence an integrated network composed of underwater, terrestrial and aerial sensors for the global protection of an asset.

Figures 1 and 2 shows a conceptual overview of the UANp network structure including the flow of data and information. The rest of the section describes the specific hardware and software used in the underwater network.

*1) UANp physical layer - the acoustic modems:* The physical layer of the UAN was supported on the acoustic modems provided by Kongsberg Maritime (KM) and specifically adapted to the task [16]. The acoustic modems operated at center frequency $f = 25.6kHz$, with a bandwidth $B = 8kHz$, source power between $173dB$ re $1\mu Pa@1m$, which was the most used during the trials, and $190dB$ re $1\mu Pa@1m$.

The modems supported two types of acoustic traffic: normal traffic that was transmitted via bidirectional Single-Input Single-Output (bi-SISO) links (between single transducer modems), and high priority, high data rate, traffic that could be exchanged using unidirectional links directed

from each individual node towards a vertical line array (VLA) of hydrophones located at the STU using a Single-Input Multiple-Output (uni-SIMO) link. The uni-SIMO layer creates a star configuration with the STU-VLA gateway located at the center, to which all the other nodes (fixed and mobile) are connected with a direct link. The uni-SIMO link does not pass via the main network stack, whereas it is handled using a leaner and parallel communication structure to increase the communication efficiency. The bi-SISO link, through which the modems operate with direct links or via multi-hops, can hence be used for routine message exchange within the network (e.g. monitoring of nodes status, environmental data exchange, etc.), whereas critical information (e.g., threat detection) can be transmitted using the high-priority uni-SIMO link to quickly reach the STU and hence the command and control center. The UANp bi-SISO physical layer is depicted in black in Figure 1, whereas the high data rate, uni-SIMO layer is represented in red.

Transmission bit rate in bi-SISO mode was $200bps$, $500bps$ and $1600bps$. Lower bit rates were based on a spread spectrum technique, whereas turbo coding was used to reach the highest bit rate. In uni-SIMO mode the maximum transmission bit rate was $8000bps$. The modems were able to provide an online CIR estimation exploiting training sequences available in every transmitted acoustic telegram, and to use this information to mitigate the Inter-Symbolic Interference (ISI).

*2) MAC and routing layers:* The lowest levels of the network were implemented directly on the modems Digital Signal Processing (DSP) board, and this included: a) Medium Access Control (MAC): implemented in the form of CSMA/CA; b) Routing: a flooding algorithm allowed for network discovery at bootstrap and in presence of topology modification events (e.g. mobile nodes movement).

The network was hence able to support retransmissions at physical layer to decrease the probability of packet loss, and was equipped with an addressing system for data packet switching and forwarding. Packets sent out in the water where repeated up-to 3 times by the transmitter, if no acknowledgement was received from the next destination node.

*3) UANp network upper layers:* On top of the bi-SISO layer, the UANp stack was completed by an IP tunneling mechanism (TUN-IP layer, in blue in Figure 1) to establish the IP connection among the nodes, by UDP as transport protocol, and by IS-MOOS as middleware level (in green in Figure 1). IS-MOOS is a publish/subscribe system, based on the MOOS framework [17], which was used, in the UAN context, to include network security mechanisms, such as integrity,

confidentiality and authentication, and to create the network interface towards the applications. Details on the specific security methologies used in UANp are reported in [11]. The use of UDP was motivated to reduce the communication overhead typical of connection oriented protocols, such as TCP. However, this makes the protocol reliability dependent on lower network layers; for example, retransmission was handled at physical level. Finally, the use of IP had the advantage of providing a standard interface towards the upper levels of the network.

Both the IP and the MOOS layers created a star-shaped network with the STU at the center (gateway or master node). In general, this might create a bottleneck for the network, since all the traffic must pass through this point, independently from the lower level configuration. In the case of the UANp network, though, due to its specific application (i.e. security and protection of critical infrastructures), this choice did not add a significant amount of overhead, since all the data had to go in any case to the C2, which was collocated with the STU. The C2 in fact had the complete control over the network behavior (e.g. node status monitoring, WAN integration, operational missions determination). The C2 presence in the network structure is depicted in purple in Figure 1.

## III. UAN11 SEA TRIAL: THRONDHEIM FJORD, MAY 2011

The UANp network described in Section II, was deployed and tested during the UAN project final sea trial, UAN11, which took place in May 2011 in the eastern part of Strindfjorden, 17 km from Trondheim, Norway. The area, with varying bathymetry ranging from 40 to 150 m, is close to commercial and touristic routes, allowing to test the system in operative conditions. The deployed network (see Figures 3 and 13) was composed of up to four fixed nodes (FNOs - Fixed NOdes) including the base station (STU-VLA), and three mobile nodes: two AUVs of e-Folaga class [14] and one additional mobile node set-up on the supporting Research Vessel (R/V) Gunnerus using a transducer located at 20m depth. The base station connected the underwater network to the land command and control station, which integrated aerial and surface additional sensors and nodes. The scenario was hence that of an integrated security system for the global protection of an asset, which, during the sea trial, was supposed as co-located with the STU. Figure 4 shows the main equipment comprised in the UANp network and deployed during the UAN11 activities.

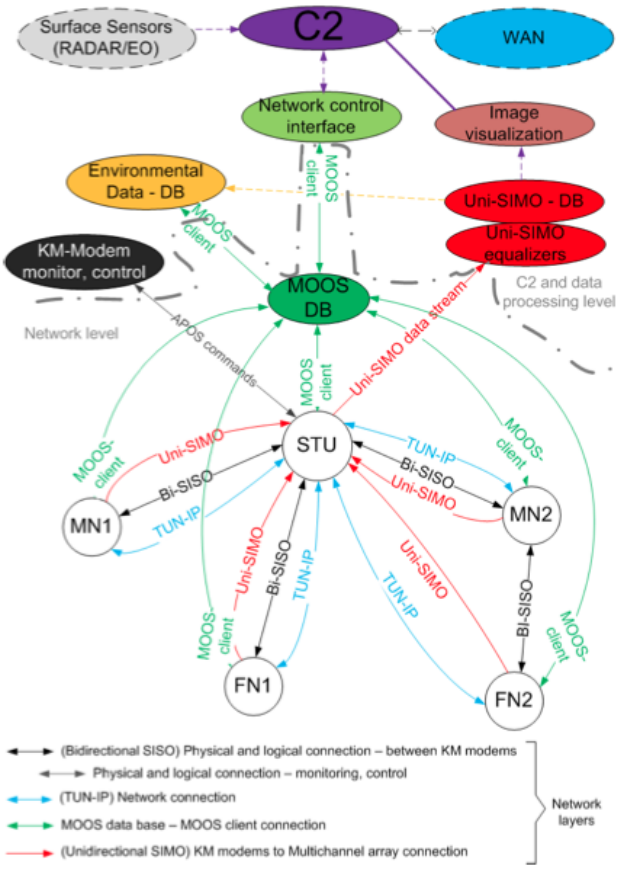


Fig. 1. UANp network structure and topology. Colored directional arrows represent the flow of data at the various levels of the network.

## IV. Environmental Data

This section describes the environment of the UAN deployment area, and reports the main environmental data gathered during the experimental activities of UAN11.

### A. *Bathymetry*

Figure 3 illustrates a three dimensional reconstruction of the bathymetry of the experimental area, including fixed nodes locations and CTD casts. The network underwater base station (STU) was located at 90.3m depth, at 800m from shore. FNO1 was positioned at about 160m from the STU at 96m depth; FNO2 was deployed in a shallower area, at 39m depth. This node was the furthest away from the STU, at a distance of about 900m. Finally, FNO3, a simplified node

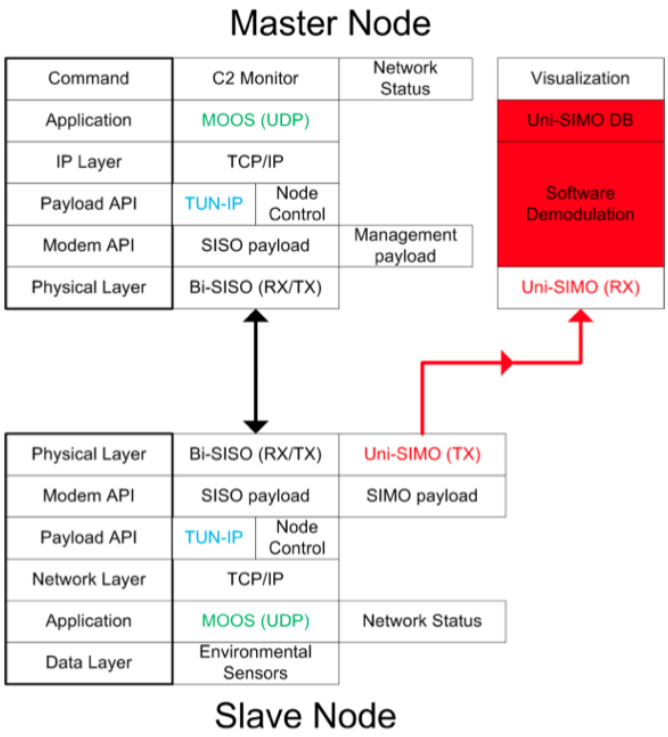


Fig. 2. Implementation of the network layers at master node (STU) and at slave nodes. The picture shows the difference between how the bi-links were handles using the entire network stack, whereas the uni-SIMO link, capable of high-data rate communications, is handled using a leaner and parallel structure to increase the communication efficiency.

implementing the network stack up to the routing, was positioned at 98m depth, 400m away from the STU.

### *B. Bottom properties*

The sediment in the region is mainly clay, whereas the underwater hills and steep regions are characterized by rock, covered with mud and clay due to the influence of rivers and tides.

### *C. Water column properties*

Conductivity, temperature and salinity data were collected daily, more times a day, using a profiler deployed from the research vessel. Locations of the CTD casts, superimposed with the bathymetry of the area, are shown in Figure 3. Additional CTDs were also taken further away from the experimental area and are not displayed in the picture. Figure 5 and Figure 6 show Sound Speed Profiles (SSP) and salinity profiles, during three days of experiment, between 25 May

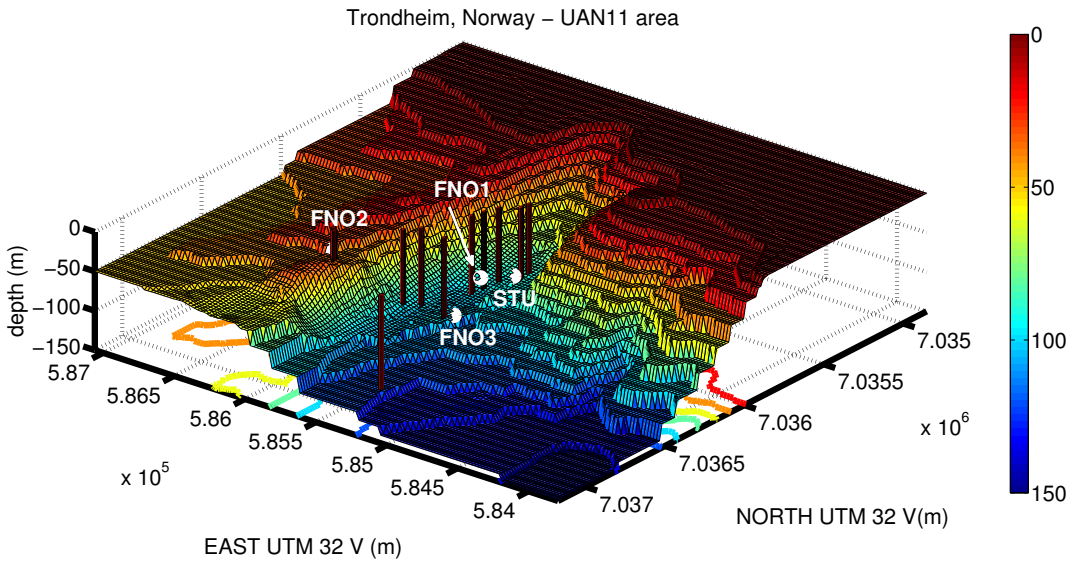


Fig. 3. UAN fixed nodes locations superimposed on the bathymetric map. CTD casts are displayed as vertical black lines at the corresponding locations.

and 27 May 2011, taken at various hours of the day. From Figure 6 it is visible the presence of fresh water in the upper layers, due to river run off and rain. As shown in Figure 5, the typical SSP profile during the days of the sea trial was characterized by a initial negative gradient, followed by a positive gradient, with the minimum at around 40m. This general behavior of the SSPs remained quite stable throughout the experiment, with the exception of May 27, when the surface layer changed (the effect of rain and wind that characterized the first days disappeared) creating a first layer with positive gradient, followed by a quasi-constant profile, and again the profile ended with the sequence of negative and positive gradient, with the minimum reached at 40m.

## V. Communication performance

The UANp network was continuously operated during the five days of the UAN11 sea trial, from 23 May to 27 May 2011. During the period, the entire network stack was fully tested, nodes were routinely added and/or removed, AUVs were seamlessly deployed within the existing fixed network, and both fixed and mobile nodes were recovered for battery recharging and then redeployed without effects on the network operation. Overall, the UANp system showed a level of robustness that went beyond expectations. The AUVs were tested both as relay nodes, and as

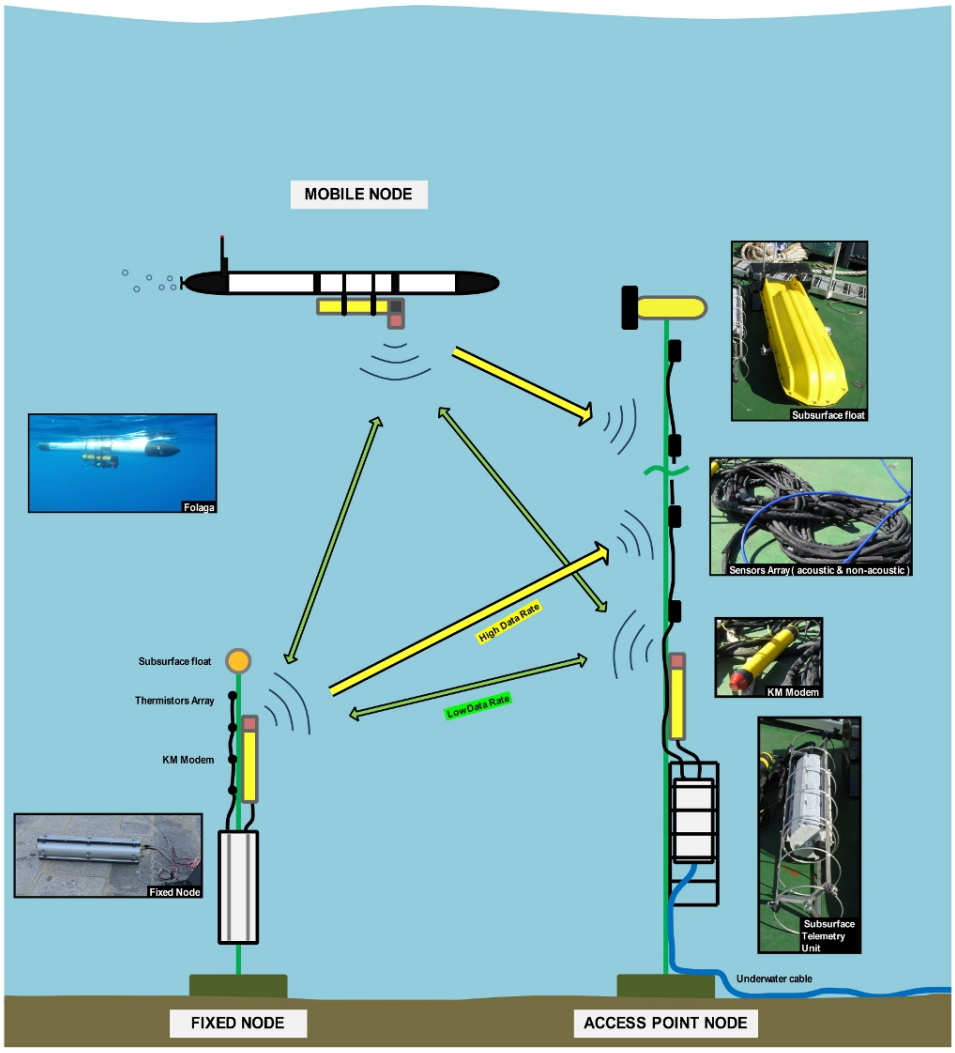


Fig. 4. UANp equipment. Fixed node composed of a vertical array of environmental sensors, a telemetry box and a modem (bottom left). Mobile node composed of an AUV and a modem (upper left). Access point node (UAN gateway) made of a VLA of hydrophones, environmental sensors, a modem and a shore connected telemetry box (right); green and yellow arrows represent SISO and SIMO links between nodes, respectively.

mobile assets of the protection system, directed acoustically from the ground C2, and/or moving autonomously when contact with the network was lost.

The first two days of the experiment were, for the most part, devoted to the network setup and to test the lowest levels of the UAN, from the physical transmission up to the MAC and routing layers. Between 23 May and 24 May 2011, TUN-IP layer and IS-MOOS were used in limited periods of time, mainly to test their integration functioning together with the other

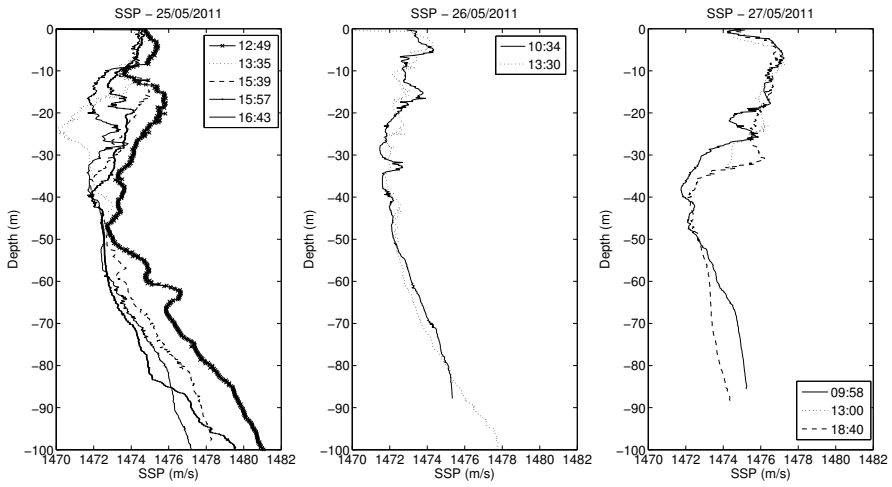


Fig. 5. Sound velocity profiles measured between May 25 and May 27, 2011

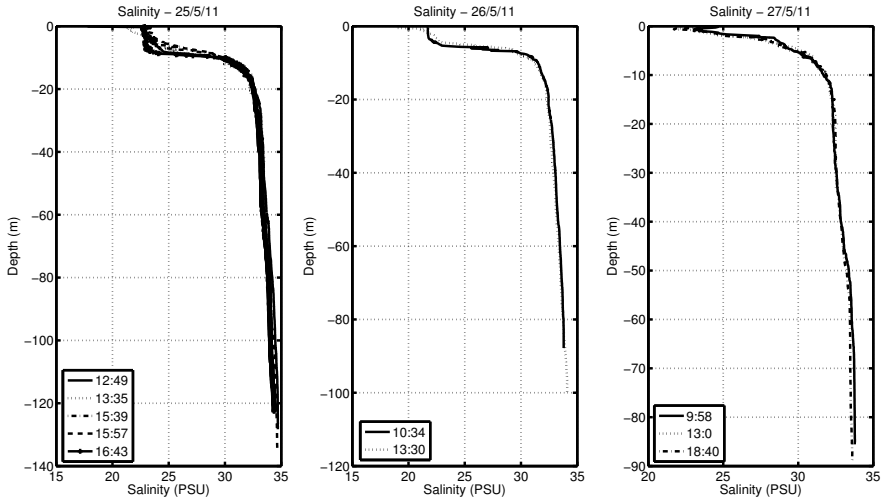


Fig. 6. Salinity profiles measured between May 25 and May 27, 2012

network components. The complete network stack was used continuously from 25 May to 27 May 2011. From May 26, network security features were activated and left on until the end of the tests. The most complex network configuration was tested on May, 27, when three fixed nodes were simultaneously in the water, together with two mobile nodes. In this case, the network was integrated within the global protection system and connected with the command and control center, which was able to receive data and send commands to the nodes/sensors.

Throughout the sea tests, the communication performance quite variable. Usually 500bps data rate was used with success in the early hours of each day, but 200bps was often necessary, especially in the afternoon.

To attempt to separate the effects of the acoustic channel from those of the system traffic, the performance during the sea tests has been evaluated at different layers using complementary metrics:

- The Channel Impulse Response (CIR), the received peak intensity, and Signal-to-Noise-plus-Interference Ratio (SNIR), as directly measured by the acoustic modems, have been used to characterize the physical layer operation.
- The Round Trip Time (RTT) and the Packet Loss (PL) have been used to evaluate the upper layers of the network, the TUN-IP layer and the MOOS middleware. The RTT has been computed as packet end-to-end delay, back and forth. The PL has been computed as the number of packets successfully received at destination, over the total number of packets sent from the source.

### *A. Physical layer performance*

Figure 7 illustrates the data (CIR, peak intensity, SNIR), as extracted from the modems logs in the transect between the STU and FNO2, on May 25. Note that there is a multipath effect in the acoustic channel that disappears in the central hours of the day, in correspondence with a decrease in SNR. The communication, on day May 25, to which Figure 7 refers, was very variable, with periods of good communication and high reception ratio, interleaved with periods characterized by high packet loss. The performance deteriorated with time, and starting from the late morning, each transmission often required several retransmissions to make the packet get through.

Computing, from the log files, the number of packets received and the number of packets lost, we have verified that the average CIR was systematically 3dB higher in case of correctly received packets. Statistically, the higher the CIR main arrival, the better the communication performance was, with a higher reception ratio at the receiver, even in presence of multipath.

Even though the SNR was typically quite low, the average of the mean of the channel impulse response was always higher when packets were received correctly. This is shown in Figure 8 for

May 25, with an average CIR of the main path in case of received packets almost 3dB higher than in the case of lost packets. This suggests that the SNR at the receiver was fluctuating above and below the threshold for correct receiving. Note also that, on May 25, the decrease in the average CIR is less evident for the second arrival.

On May 26 the same situation occurred, however from 11.30 to 12.30 hrs., the network was modified with FNO3 used as relay to reach FNO2 through a multi-hop link. Everything else being equal, this had the effect of immediately improving the communication performance between STU and FNO2, with a subsequent degradation as soon as the multihop link was removed. This observation seems to rule out the possibility of degradation due to increased network traffic. The CIR contour map and SNIR are reported in Figure 9, while the comparion between the CIR mean and the reception ratio is represented in Figure 10. Again, the higher the SNR the better the communication was, regardless from the presence of period of multipaths. To better highlight the visible increase in communication performance during the multihop period, Figure 11 reports a sequence of successful pings executed, when FNO3 was used as a relay, within a long period of unsuccessful communication using the direct link STU-FNO2. Note that in Figure 11, lost pings can correspond to packets that were lost in the water or to packets whose RTT exceeded the timeout period that was set at 120s. This design was necessary to force issuing the next ping request. As such, a lost ping in Figure 11 indicate bad channel conditions, long queue backlogs, or both at the same time, since the former leads to the latter.

### *B. TUN-IP and MOOS performance*

This section analyses the performance of the upper layers of the network during the UAN11 sea trial. The TUN-IP layer represents the link between between the physical layer and the upper parts of the network, i.e. transport, middleware and applications. Its performance hence turns out to be very important to understand the UANp performance at network level.

Figure 12 shows the IP layer packet delay, as measured in the link between the STU and FNO2 (see Figure 12a and 12b) from May, 25 to May 27. This was the link where the greatest number of packets was exchanged.

During the period of experimentation, observed isolated packet delays increased up-to 500sec with a total packet loss of about 40%, from STU to FNO2, and of 42.9%, from FNO2 to STU. However, most of the data was received with a delay between 3 and 20 seconds. High packet

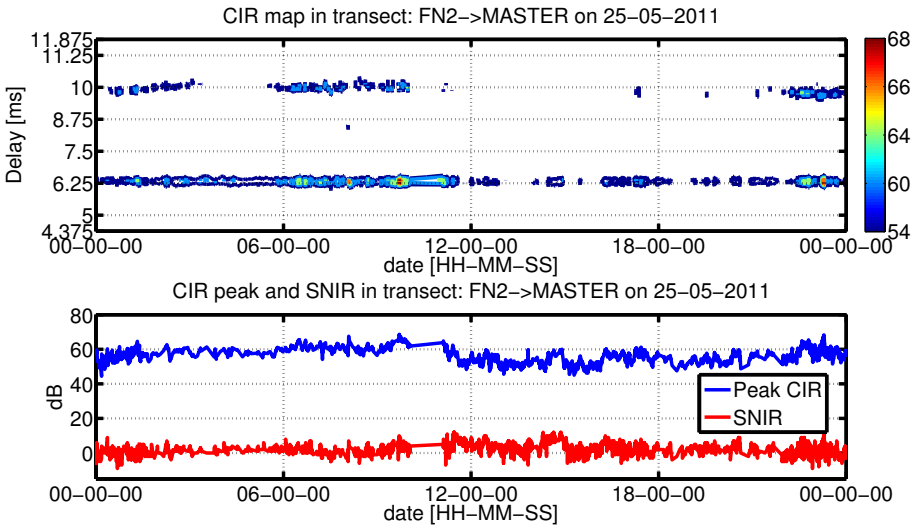


Fig. 7. May 25, transect between FNO2-STU: CIR contour map in dB (top), denoised using a Constant False Acceptance Ratio test. CIR peak and SNIR values in dB (bottom).

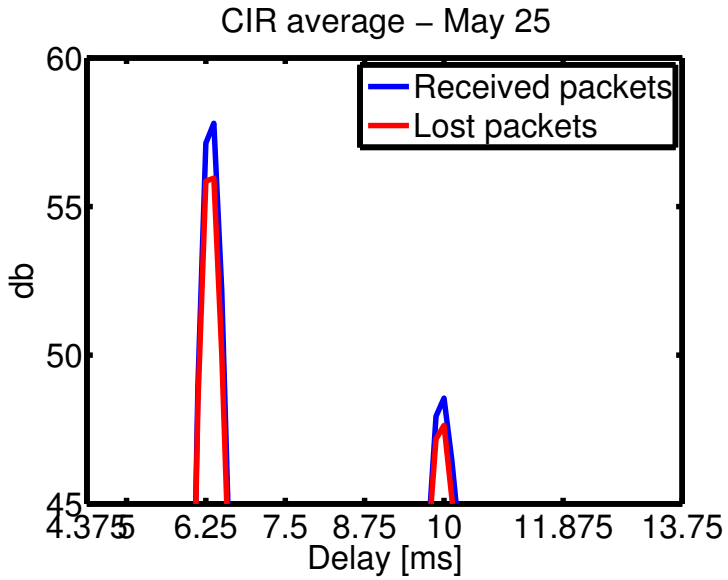


Fig. 8. May 25, transect between FNO2-STU: the average CIR value of the main path, for received packets is 3db higher than the average CIR in the case of lost packets.

delay was due mainly to queue backlog and buffering. It is worth pointing out that no feedback was available at TUN-IP layer on the success of the delivery; packets would simply be discarded after being sent out to the acoustic modems via serial line. If for any reason the remote node did

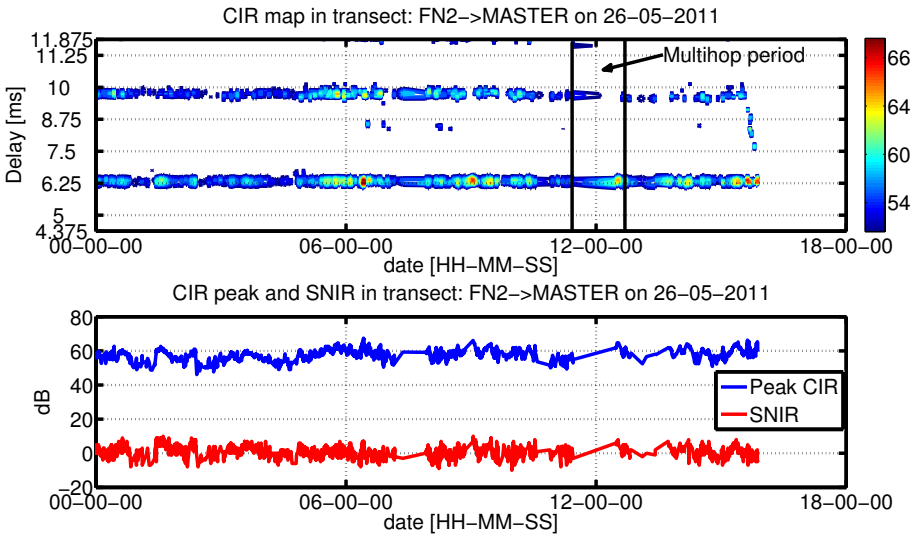


Fig. 9. May 26, transect between FNO2-STU: CIR contour map in dB (top), denoised using a Constant False Acceptance Ratio test. CIR peak and SNIR values in dB (bottom). A multihop link was used to reach FNO2 from STU from 11.30 to 12.30 hrs. It is visible the gain in the impulse response when multihop was used.

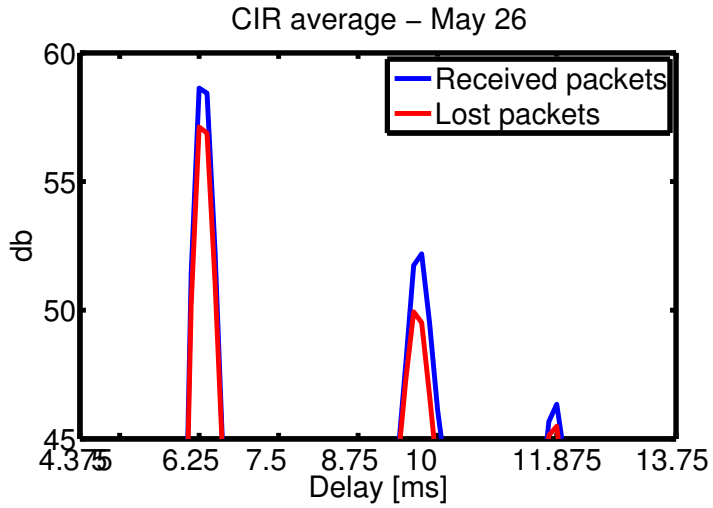


Fig. 10. May 26, transect between FNO2-STU: the average CIR value of the main path for received packets is 2.5dB higher than the average CIR in the case of lost packets.

not respond to specific control commands, the link was assumed as broken by the transmitter, which considered the packet as lost before reception. In several occasions, however, as came out after the sea trial, in post-processing, the remote node was indeed able to receive the incoming

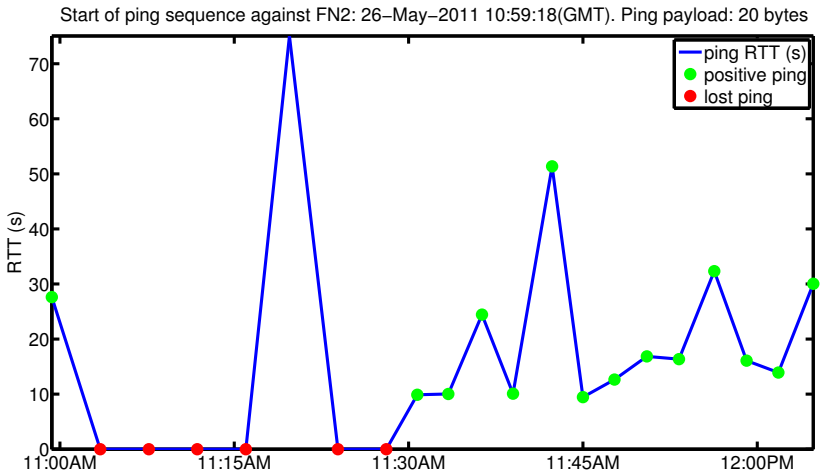


Fig. 11. RTT of pings of 20 bytes sent from the STU to the FNO2. Within a period of direct unsuccessful communication between the nodes, from 11.30am, the communication was routed for about 1 hr via FNO3. The picture shows a visible increase in performance that corresponds to the new path.

packet, whereas it was its reply to be lost, and never received by the first node.

Middleware performance, in terms of PL and RTT (i.e. end-to-end delay, back and forth) is summarized in Tables I and II for the period May, 23 - 27, per each node of the network. Average PL varied between 0-68% approximately, remaining in most cases between 30% and 50%; average RTT went from 7s to 240s, remaining between 60s and 120s most of the time. This values sum up the delays of the entire network stack, both at source and at destination. Note that, due to the loss of the node during recovery, RTT statistics for FNO1 on 23 and 24 May are not available even though the node was operative in the period.

### *C. UANp operational example*

On May 27, the most complex network was in the water. The UAN was composed of three fixed nodes (STU, FNO2 and FNO3) plus two mobile nodes. The network was also integrated into the global protection system, composed of underwater, aerial and terrestrial sensors monitored and controlled by a Command and Control center (C2). In this context, a complex anti-intrusion scenario was set-up to verify the capability of the system to detect and respond to threats. Within this scenario, the e-Folaga AUVs were used as mobile assets of the protection system, i.e. as reactive means acoustically controlled by the C2 to respond to intrusions, and kept mostly on

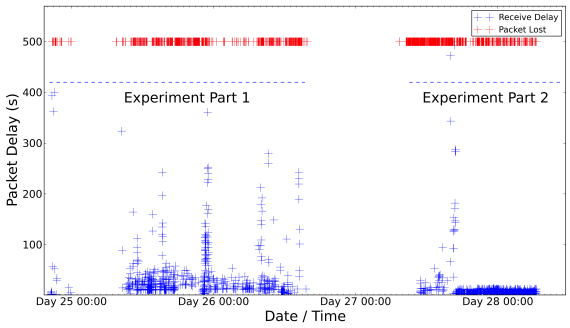


(a) from STU to FNO2

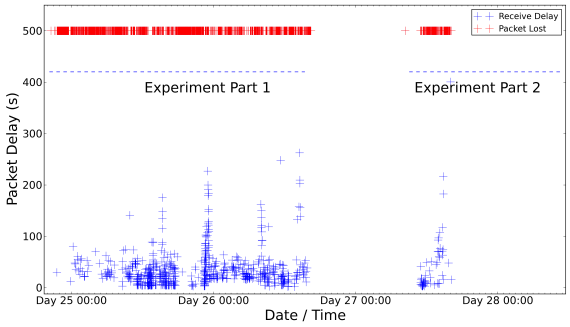


(b) from FNO2 to STU

Fig. 12. Delays as computed at IP layer between the STU and FNO2. Total packet loss was 40%, from STU to FNO2, and 42.9%, from FNO2 to STU. Most of the data was received with a delay of up-to 3 to 20 seconds. High packet delay was due to a buffering system present on the nodes.

surface. To this aim, when one of the fixed nodes detected a possible intrusion, the C2 sent one of the AUVs to the point of intrusion to investigate the area. When the vehicle arrived to the designated point, however, it found itself out of the network, without acoustic connectivity. For this reason, after detecting the poor level of communication, the mission planner onboard the AUV, autonomously planned a new mission to move closer to the STU. Note that, the vehicle was not equipped with an acoustic model able to predict its movement towards poorly covered areas, whereas the mission planner was only able to track the packet loss at application level to identify when the AUV was in regions characterized by poor communication conditions. This scenario is represented in Figure 13 in terms of the trajectories followed by the AUV during its mission. The picture also reports the main mission phases.

| *Date* | *Node* | *Average Paket Loss (%)* |
|---|---|---|
| 23 May 2011 | FNO1 | 0 |
| | FNO2 | 29.37 |
| 24 May 2011 | FNO1 | 11.11 |
| 25 May 2011 | FNO2 | 58.75 |
| 26 May 2011 | R/V | 32.76 |
| | FNO2 | 54.76 |
| 27 May 2011 | Folaga1 | 18.31 (until 2.00 pm) |
| | Folaga2 | 49.64 (after 3.00 pm) |
| | R/V | 40.58 |
| | FNO2 | 68.38 |

TABLE I

PACKET LOSS AT MIDDLEWARE LEVEL PER DAY PER EACH NODE.

| *Date* | *Node* | *Average RTT (s)* |
|---|---|---|
| 23 May 2011 | FNO2 | 17.39 |
| 25 May 2011 | FNO2 | 58.71 |
| 26 May 2011 | R/V | 248.91 |
| | FNO2 | 54.39 |
| 27 May 2011 | Folaga1 | 38.81 (up to 2.00 pm) |
| | Folaga2 | 112.95 (after 3.00 pm) |
| | R/V | 35.28 |
| | FNO2 | 107.42 |

TABLE II

ROUND TRIP TIME AT MIDDLEWARE LEVEL PER DAY PER EACH NODE.

## VI. ACOUSTICS PROPAGATION AT UAN11

In order to test if indeed there was a degradation in channel performance due to the variation in the environmental conditions (i.e., the SSP), the Bellhop ray model was run in correspondence with the SSP as measured during the same day.

The numerical simulations has been done computing the main path impulse response and the incoherent TL (1) to analyze the results of the sea trial:

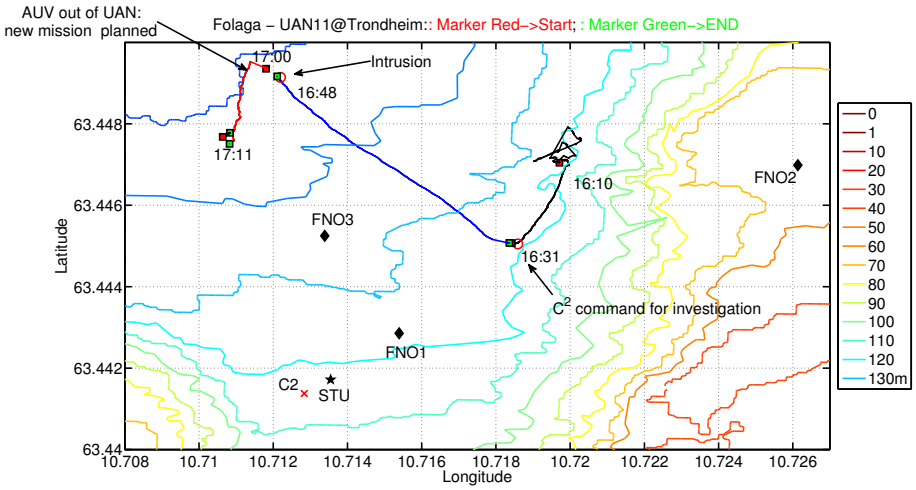


Fig. 13. e-Folaga trajectories on May 27, 2011. The vehicle was acoustically controlled by the command and control and moved to investigate a possible intrusion. The vehicle found it self without acoustic connectivity (h. 17.00) and planned an autonomous mission to move closer to the STU (red line), where it was able to re-enter into UAN. The point of intrusion was located in the upper-left part of the picture (63.449, 10.712).

$$TL(r, r_s) = -20Log_{10}\left|\frac{p^{(I)}(r,z)}{p_0(r_s)}\right| \tag{1}$$

where the incoherent pressure field $p^{(I)}$ is computed as:

$$p^{(I)}(r,z) = \left[\sum_{j=1}^{N(r,z)} |p_j(r,z)|^2\right]^{1/2} \tag{2}$$

where $r$ is the horizontal distance, $z$ is the depth, $N(r,z)$ denotes the number of eigenrays contributing to the field at a particular receiver position, $p_j(r,z)$ is the pressure due to that eigenray, and $p_0(r_s)$ is the pressure produced at a distance of 1m from the same source in an infinite, homogeneous medium [18].

Equation (1) is used here to assess in a qualitative way the relative variation of SNR in the channel, as the TL is linked to the SNR through the well known sonar equation (3), [18]:

$$SNR = SL - TL - (N + RL) \tag{3}$$

where $SL$ is the source level, $N$ is the ambient noise level and $RL$ is the reverberation level.

In what follows we give more emphasis on the analysis of May 25, 2011, when the largest number of CTDs was taken within the same day, permitting to have a better picture of the

changes in the TL as the environment changed. Further simulations have been performed on May 27, 2011 for the acoustic links between the STU and the mobile nodes, and their results are also reported.

### *A. Changes in CIR and TL between STU and FNO2 on May 25*

The variation of the CIR and of the incoherent TL, as computed by BELLHOP with varying SSPs, on May 25, in the transect between the STU (source) and FNO2 (receiver), is reported in Figure 14 and 15, respectively. The model indeed predicts a decrease in the intensity of the main arrivals and a consequent increase in the Transmission Loss (TL) at FNO2 developing within the day as observed in the experimental data. Note that the CIR and the TL shown in Figure 14, are used as an indication of qualitative variation of the response of the acoustic channel. It is also worth pointing out that the absolute delay values in Figure 14 do not correspond to those measured in the field due to a time normalization executed by the acoustic modems before recording the CIR. However, the time difference between the first and the second main peak in the computed CIR are compatible with those measured in the field, taking into account the uncertainty (greater than 1m) in the localization of the nodes.

The variation in the communication channel is due to the afternoon change in the SSP, with the presence of a higher gradient in the lowest part of the profile. This modifies the ray pattern moving an important part of the energy upwards, and hence away from the receiver (FNO2), determining a corresponding increase in the TL, and a decrease in the received signal. To better highlight the difference in the TL at the FNO2 location, Figure 16 reports, on the left, the TL values saturated between 50 and 55dB and corresponding to the SSP variations, and on the right, the corresponding ray paths. The figures show the energy bounced off the bottom away from the FNO2.

This kind of slight change in the bottom part of the SSP has been registered often in the afternoon during the sea tests and it was usually accompanied by a rapid deterioration in the communication performance between the STU and FNO2. There was no further CTD available after 16.34 hrs., and this lack of information prevented the attempt of modeling the observed performance recovery after 17.30 hrs.

The predicted CIR shows a decrease in the first arrival energy while the second main arrival does not show a significant variation. While there is discrepancy between the relative amplitudes

of the first and second arrival, as predicted by BELLHOP and as measured in the field, the model is able to predict the trend of variation of both first and second arrival as seen in the experimental data.

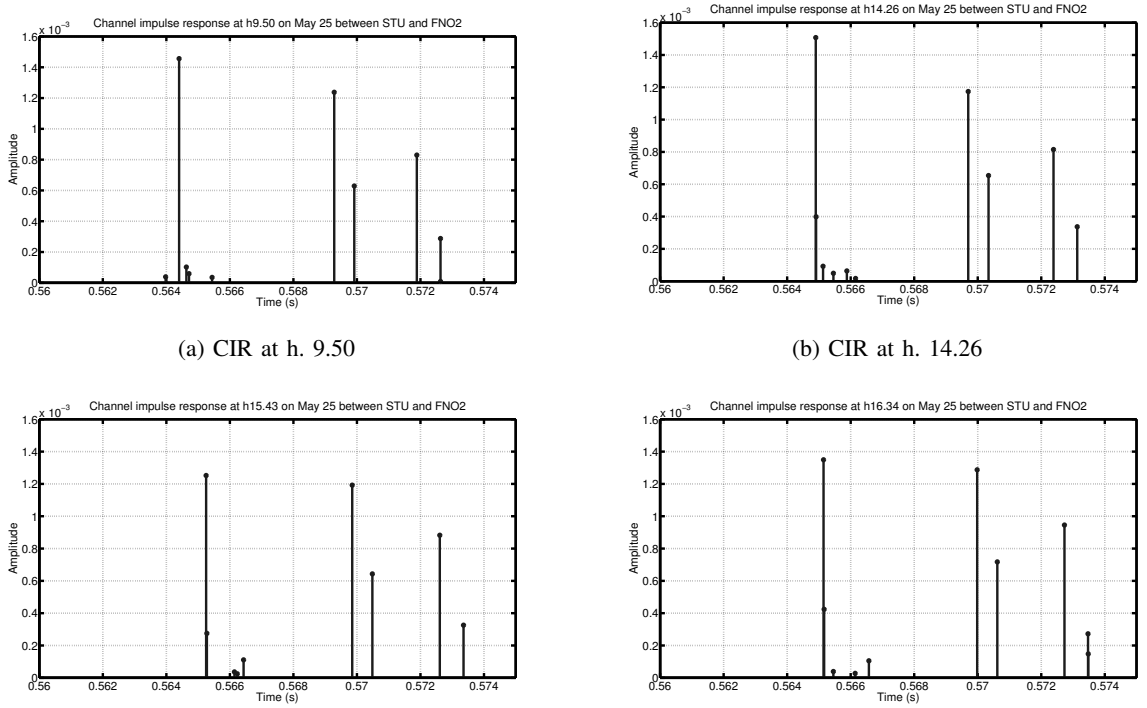


(a) CIR at h. 9.50

(b) CIR at h. 14.26

(c) CIR at h. 15.43

(d) CIR at h. 16.34

Fig. 14. Evolution of the channel impulse response between STU (source) and FNO2 (receiver), as calculated by BELLHOP with varying sound speed profiles at various hours on May 25, 2011. The STU is at 80m depth, and FNO2 is located at 40m depth. It is visible the decrease of the main paths after h15.43.

The variation in the TL due to the afternoon change in the SSP appears also at shorter distances, as in the case between STU and FNO1, which are less than 200m apart. However, at such distances, where the SNR is in any case well above the reception threshold, small variations in TL are not critical to influence the overall ability to communicate. In these conditions, it becomes more important the impact of the network itself (e.g. MAC, multi-hops, etc.) to justify the variation in the communication performance.

As a final case, the anti-intrusion scenario described in the previous section and in Figure 13, and tested on May 27, has been simulated with BELLHOP to evaluate the incoherent TL corresponding to the two phases of the AUV mission: a) before receiving the command from

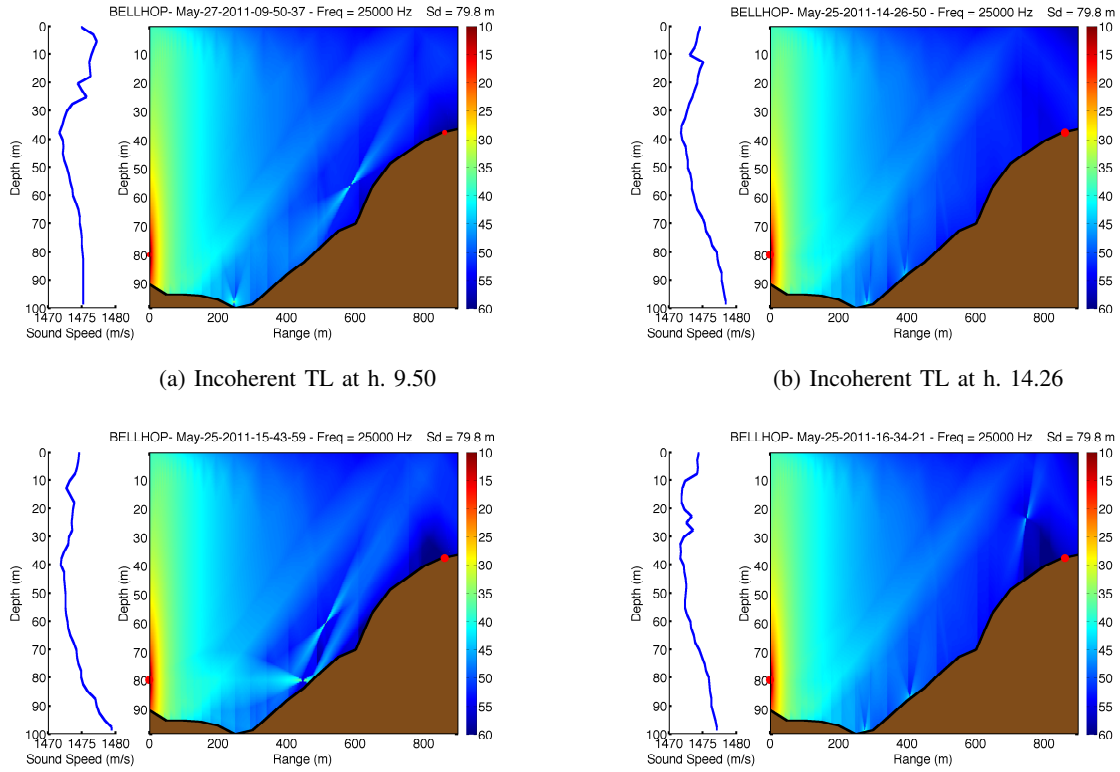


(a) Incoherent TL at h. 9.50

(b) Incoherent TL at h. 14.26

(c) Incoherent TL at h. 15.43

(d) Incoherent TL at h. 16.34

Fig. 15. Evolution of the incoherent TL, as calculated by BELLHOP with varying sound speed profiles at various hours of the day (May 25, 2011). The STU (source) is at 80m depth, and FNO2 (receiver) is located at 40m depth. Both nodes are represented as red circles at the corresponding depths. Note however that the positions indicated by the circles are only indicative of the true positions of the nodes in the water.

the C2, and b) once it reached the intrusion point. Figure 17 shows the results obtained in the two cases. The distance from the STU, together with the change in bathymetry, resulted in an important increase in the TL (about 8 dB more) and the consequent degradation of the communication.

## VII. Observations and Remarks

On the basis of the results presented, several comments can be made on the network performance at different levels.

- The acoustic modems used in the UANp operations appeared to be quite robust against multipaths. In the UAN11 scenario, where the main arrival was well separated, the KM modems were effectively able to exploit their online computation of the CIR to mitigate

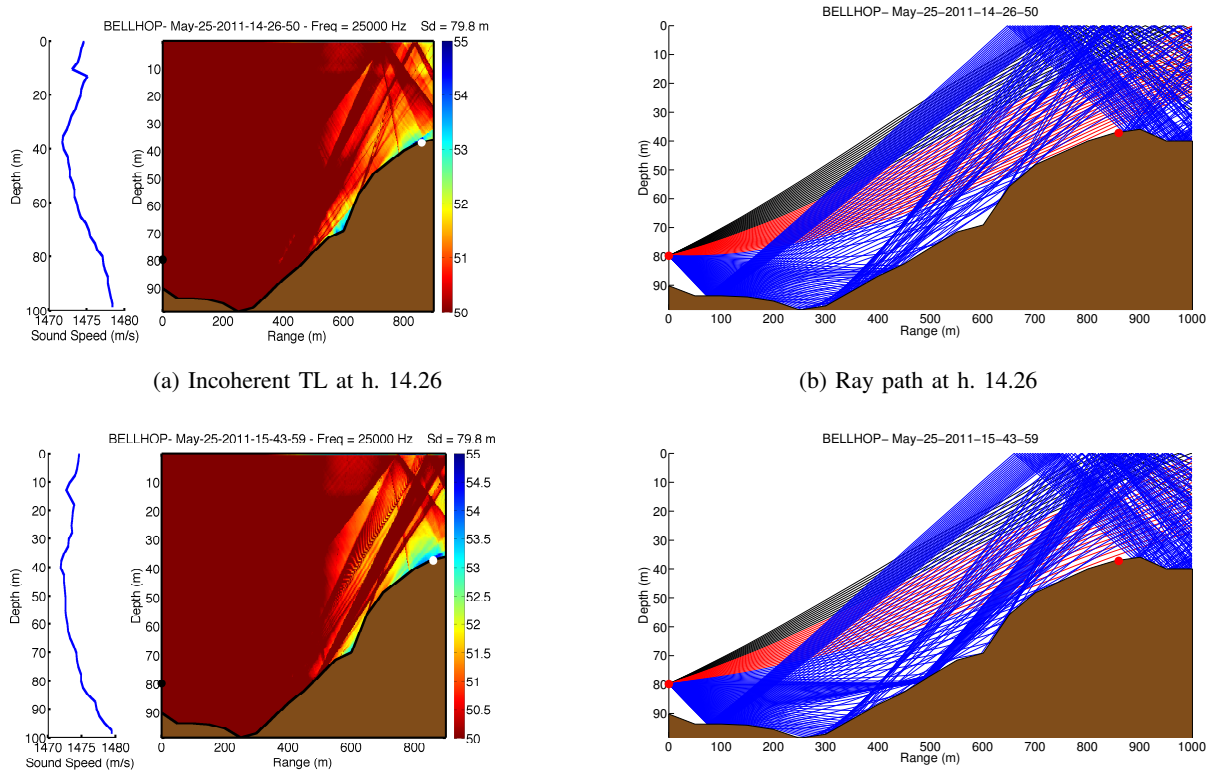


(a) Incoherent TL at h. 14.26

(b) Ray path at h. 14.26

(c) Incoherent TL at h. 15.43

(d) Ray path at h. 15.43

Fig. 16. Left: Incoherent TL saturated between 50 and 55dB to highlight its variation at the FNO2 location. The variation is due to the change in the SSP on May 25, 2011. Note that the position of the transmitter is indicated by a black circle; the receiver by a white circle. Right: Ray paths in the transect between the STU and FNO2. Note that due to the bathymetry shape no direct path exists between the source and the receiver.

multipaths effects, increasing the probability to correctly receive a packet. On the contrary, they seemed more fragile with respect to SNR decrease. Trondheim fjord communication conditions were difficult throughout the days of experimentation, with a fairly low SNR (less than 10dB). In this conditions, even small variations of the SNR implied great changes in the communication capabilities.

- The big delays experienced at the upper levels of the network cannot only be caused by the packet propagation in the water, while several concurrent effects were interacting in producing such performance.

  First of all, if a packet was lost in the water channel due to noise or collisions, or signal fade, the acoustic modems would attempt retransmission up to three times before stopping

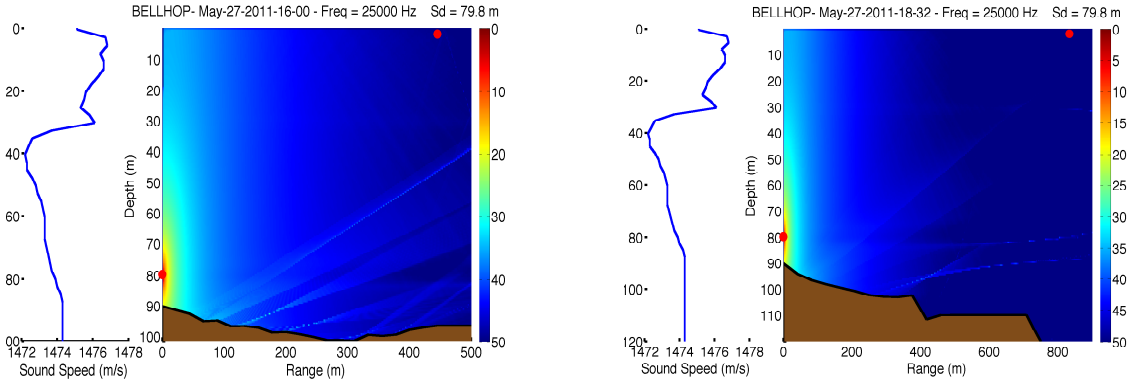


(a) Incoherent TL at h. 16.00

(b) Incoherent TL at h. 18.00

Fig. 17. Transmission loss between the STU and the Folaga (both nodes are represented as red circle). Top: early in the afternoon; Bottom: late in the afternoon when the vehicle found itself out of the network. The difference in TL between the two cases is about 8 dB. The STU and the Folaga are represented as red circles at the corresponding depths.

any further attempt with that packet. Furthermore, the average size of a MOOS packet was $150bytes$, which is above the size available to be transmitted by the acoustic modem as a single acoustic telegram. As a result, MOOS packets were often fragmented into several frames, each one transmitted separately and with its own acknowledgment and, if necessary, retransmission.

- In the case of smaller packets, as ping packets (see Figure 11), large delays were mostly due to queue backlog, as in the case of new ping packets fed into the system before the former was finished, or in the case of MOOS data traffic simultaneously present with ping traffic. Other delays might also have been caused by the operation of the protocol CSMA/CA. According to this protocol each node is able to detect a busy channel (i.e. another node is already transmitting) to prevent collisions. In this case, the node backs off for a random time before verifying the availability of the channel for transmission. However, in presence of high propagation delays typical of underwater acoustic networks, one device might not detect that another one has already started the transmission, resulting in a simultaneous transmission and a collision. This might become even more important in the case of multi-hop connections, when the packets have to travel through more than one link to get to their destinations. As a result, the overall network performance, including IP, was strongly related to the acoustic channel conditions, i.e. relative locations between the nodes, mobile nodes

movement, and to the particular traffic which was undergoing into the network layers, as for example in situations of network congestions.

- The computation of the TL and of the CIR estimate by standard acoustic codes is in agreement with the communication performance observed in the field, at least in a qualitative manner. In the UAN scenario, the communication was dominated by the SNR, and in this case, the TL seems to be a good indicator of performance variations. Even though it is clear that the overall performance of the network depends on the interplay occurring at different layers, the use of the TL or similar channel indicators, can provide useful information that can be effectively used to adapt the behaviour even at the highest levels of the network.

## VIII. Conclusion

This work analyzed the performance of the acoustic underwater network (UANp) deployed within the FP7 UAN project, during the UAN11 experimental activities held in May 2011, off the coast of Trondheim, Norway. The network, composed of four fixed nodes, two AUVs, and one mobile node mounted on the supporting research vessel, was continuously operated for five days, and integrated into a global protection system.

The paper reports the details of the communication and network protocols employed.

UANp in the field performance has been presented, pointing out the relations between the various network layers in explaining the overall communication results. Results from the experimental activities are reported using different metrics at different layers: the physical layer performance is reported in terms of CIR, received peak intensity, SNIR as measured online by the acoustic modems; the network upper layers performance is characterized in terms of probability of packet loss and round-trip-time.

The network communication was affected by the changes in the acoustic channel, and by the network structure itself, e.g. MAC protocol, multi-hops, etc. In the UAN scenario, variation in the SNR appears to be more important in explaining the changes in communication performance. The receivers could cope with multipath, exploiting their own ability in estimating the channel impulse response, but were more fragile with respect to SNR decrease. Furthermore, the influence of the acoustic channel on the network appears to be more important on longer distances, when

the use of multi-hops to guarantee connection showed a clear increase in performance.

Environmental channel modeling with Transmission Loss and CIR estimate computed with Bellhop ray-tracing code indicates that TL computation by standard methods can qualitatively predict relative variations in communication performance. It is underlined that Bellhop predictions are qualitatively in agreement with the observed communication performances. This indicates, that, at least in the cases where the communication performance is dominated by SNR, the computation of the TL with standard ray models can be used as a relative indicator of performance variation.

Even though the network performance was indeed dependent on several concurrent effects, spread out at the various network levels, it appears that the use of the TL, together with other channel performance indicators might give insights that can be useful even at the highest level of the network (e.g. to move mobile nodes to improve the communication, etc.).

## ACKNOWLEDGMENT

This work has been supported in part by European Union under the FP7 UAN Underwater Acoustic Network project, Grant n. 225669. The authors wish to thank the R/V Gunnerus captain and crew for their support during the UAN11 experimental activities, and the entire UAN project team.

## REFERENCES

[1] J. Heidemann, M. Stokanovic, and M. Zorzi, "Underwater Sensor Networks: Applications, Advances, and Challenges," *Phil. Trans. R. Soc. A*, vol. 370, no. 1958, pp. 158–175, May 2012.

[2] S. Petillo, H. Schmidt, and A. Balasuriya, "Constructing a distributed auv network for underwater plume-tracking operations," *Int. J. Distributed Sensor Networks*, 2012.

[3] I. F. Akyildiz, D. Pompili, and T. Melodia, "Underwater acoustic sensor networks: research challenges," *Ad Hoc Networks*, vol. 3, no. 3, pp. 257–279, May 2005.

[4] J. Heidemann, U. Mitra, J. Preisig, M. Stojanovic, M. Zorzi, and L. Cimini, "Guest Editorial - Underwater Wireless Communication Networks," *IEEE Journal on Selected Areas in Communications*, vol. 26, no. 9, pp. 1617–1619, Jul. 2008.

[5] M. Chitre, S. Shahabudeen, L. Freitag, and M. Sjotanovic, "Recent Advances in Underwater Acoustic Communications & Networking," pp. 1–10, Jul. 2008.

[6] D. Pompili and I. F. Akyildiz, "Overview of Networking Protocols for Underwater Wireless Communications," *IEEE Communication Magazine*, pp. 1–6, Jan. 2009.

[7] J. Rice, "SeaWeb acoustic communication and navigation networks," 2005.

[8] L. Freitag, M. Grund, S. Singh, J. Partan, P. Koski, and K. Ball, "The whoi micro-modem: an acoustic communications and navigation system for multiple platforms," in *OCEANS, 2005. Proceedings of MTS/IEEE*, 2005, pp. 1086–1092.

[9] T. Schneider and H. Schmidt, "Unified command and control for heterogeneous marine sensing networks," *Journal of field robotics*, vol. 27, no. 6, pp. 876–889, 2010.

[10] C. Petrioli, R. Petroccia, and J. R. Potter, "Performance evaluation of underwater mac protocols: from simulation to at-sea testing," in *Proc. of the IEEE Oceans-11 Conf., Santander, Spain*, 2011.

[11] A. Caiti, V. Calabro, G. Dini, A. Lo Duca, and A. Munafo, "Secure Cooperation of Autonomous Mobile Sensors Using an Underwater Acoustic Network," *Sensors*, vol. 12, no. 2, pp. 1967–1989, Feb. 2012.

[12] A. Caiti, T. Husoy, S. M. Jesus, I. Karasalo, R. Massimelli, A. Munafo, T. A. Reinen, and A. Silva, "Underwater Acoustic Networks: The FP7 UAN Project," in *9th IFAC Conference on Manoeuvring and Control of Marine Craft (MCMC)*, Jul. 2012, pp. 1–6.

[13] F. Zabel, C. Martins, and A. Silva, "Design of a uan node capable of high-data rate transmission," *Sea Technology*, vol. 52, no. 3, pp. 32–36, March 2011.

[14] A. Caiti, V. Calabrò, G. Dini, A. L. Duca, and A. Munafò, "Mobile underwater sensor networks for protection and security: field experience at the uan11 experiment," *Journal of field robotics*, accepted for publication, 2012.

[15] M. B. Porter, "The BELLHOP Manual and User's Guide," Tech. Rep., Feb. 2011.

[16] T. Husoy, M. Pettersen, B. Nilsson, T. Öberg, N. Warakagoda, and A. Lie, "Implementation of an underwater acoustic modem with network capability," in *IEEE Oceans Conf.*, Apr. 2011, pp. 1–10.

[17] O. M. R. Group, "The MOOS Cross Platform Software for Robotics Research," Tech. Rep., Dec. 2011.

[18] F. B. Jensen, W. A. Kuperman, M. Porter, and H. Schmidt, *Computational Ocean Acoustics*, R. T. Beyer, Ed. Springer, Feb. 1994.